

# SWITCHING STRATEGIES IN DIRECT TORQUE CONTROL OF INDUCTION MACHINES

## STRATEGIES DE COMMUTATION POUR LE CONTROLE DIRECT DE LA COUPLE DES MACHINES A INDUCTION

### Abstract

AC drives based on direct torque control of induction machines allow high dynamic performance to be obtained with very simple control schemes. For a prefixed switching strategy, the drive behaviour, in terms of torque and current ripple, switching frequency and torque response, is quite different at low and high speed. In this paper a detailed discussion of some possible voltage vector selection criteria is carried out. Furthermore, a control system is presented in which the good drive performance is accomplished in steady state as well as under transient conditions by the combination of different switching strategies. The selection is based on the value of mechanical speed or stator flux angular frequency. The control scheme has been implemented using a DSP-based hardware. Results of experimental tests are also presented.

### Introduction

In three-phase induction motor drives a complete decoupling of flux and torque control variables is usually required. The field oriented control is an appropriate method to meet these requirements. The torque command is generated from speed-loop controller or directly by the user, such as in traction drives for electric vehicles. The flux command is selected according to operation requirements, i.e. field weakening operation to achieve a wide speed-range or flux regulation in accordance with load conditions to minimise motor losses.

In most control strategies the input commands are torque and flux, whereas the output commands are three-phase reference currents. Then, the power converter has to be able to force any desired current waveforms into stator windings. For this purpose, current controlled voltage-source inverters can be used. In order to obtain good performance, the desired current waveform has to be well approximated leading to high switching frequency.

In a previous paper [1] stator flux components are utilised as controlled variables, in the same way as in field oriented control schemes the stator current components are utilised. The use of stator flux components as controlled variables allows the saturation effects in detuned operation to be reduced. Furthermore, a change in rotor flux command is followed with a time constant which is much lower than that involved in stator current control.

In reality, voltage-source inverters can produce only seven discrete voltage space vectors and properly selecting one of these vectors at any sampling period, it is possible to control independently stator flux and torque by using hysteresis controllers [2], [3]. This control technique, usually called Direct Torque Control (DTC), results in high performance AC servo systems which require very simple control schemes (Fig. 1).

Furthermore, utilising these control schemes, the requirements of current regulator, proportional-integral control of flux and torque, PWM pulse width creation are eliminated. As a consequence the dynamic performance of the drive system can be improved. In general, the DTC method is based on the control of torque and stator flux, but the rotor flux can be also assumed as reference. In this case the highest pull-out torque can be achieved [4].

D. Casadei, G. Grandi, G. Serra and A. Tani

Università degli Studi di Bologna - Facoltà di  
Ingegneria - Istituto di Elettrotecnica  
Viale Risorgimento, 2  
40136 BOLOGNA - ITALY

### Keywords

- Induction Motor Drives
- Direct Torque Control
- DC/AC Power Converter Control
- Switching Strategy Optimisation
- Digital Control Systems

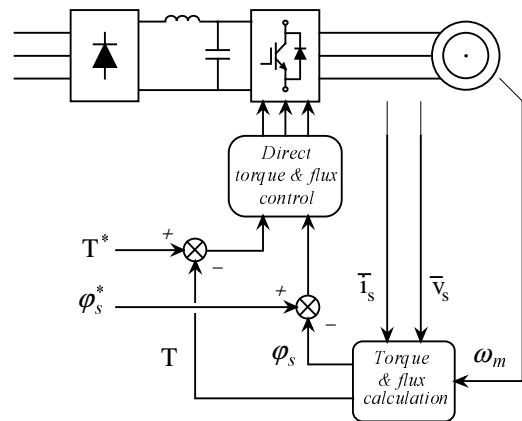


Fig. 1 - Block diagram of Direct Torque Control system.

Different switching strategies can be employed to control the torque according to whether the flux has to be reduced or increased. Each strategy affects the drive behaviour in terms of torque and current ripple, switching frequency and two- or four-quadrant operation capability.

In this paper the analysis is concerned with a control scheme in which, according to the switching capabilities of voltage source inverters, the selection of the switching configuration is made, step-by-step, in order to maintain the stator flux and torque within the limits of two hysteresis bands. A new control technique which utilises different switching strategies according to prefixed speed ranges is presented. The advantages associated to this control technique are discussed and some experimental results showing the transient response of the torque control are given.

### Direct torque control principles

A general system configuration of DTC scheme is represented in Fig. 1. In this system the instantaneous values of flux and torque can be calculated from stator variables and mechanical speed or utilising stator variables only. Stator flux and torque can be controlled directly and independently by properly selecting the inverter switching configurations.

In voltage source inverters, eight switching combinations can be selected, two of which determine zero voltage vectors and the remaining generate six equally spaced voltage vectors having the same magnitude, as shown in Fig. 2. The stator voltage equation, written in terms of space vectors, is

$$\frac{d\vec{\varphi}_s^s}{dt} = \vec{v}_s^s - R_s \vec{i}_s^s \quad (1)$$

Assuming the voltage drop  $R_s i_s$  small, the head of the stator flux  $\vec{\varphi}_s^s$  moves in the direction of the stator voltage  $\vec{v}_s^s$  at a speed proportional to the magnitude of  $\vec{v}_s^s$  according to

$$\Delta\vec{\varphi}_s^s \equiv \vec{v}_s^s \Delta t \quad (2)$$

where  $\Delta t$  is the period in which the voltage vector is applied to stator windings. Selecting step-by-step the voltage vector appropriately it is then possible to drive  $\vec{\varphi}_s^s$  along a prefixed track curve.

From the general equations of induction machines referred to a rotor reference frame, the following equation can be derived

$$\vec{\varphi}_r^r = \frac{M}{L_s} \frac{1}{1 + p\sigma\tau_r} \vec{\varphi}_s^r \quad (3)$$

This equation clearly shows the nature of rotor flux dynamic response for changes in stator flux.

In steady-state conditions, for sinusoidal waveforms, the stator flux vector has to describe a circular trajectory. However, owing to the switching process, the stator flux vector locus is irregular, while the rotor flux vector locus is practically a circle owing to the first order, low-pass filtering action expressed by (3). In steady-state conditions the stator and rotor flux vectors have the same angular speed and the angle  $\vartheta_{sr}$  between these vectors determines the electromagnetic torque value, according to the following expression

$$T = P \frac{M}{\sigma L_s L_r} \vec{\varphi}_s^r \cdot j\vec{\varphi}_r^r = P \frac{M}{\sigma L_s L_r} \varphi_s \varphi_r \sin \vartheta_{sr} \quad (4)$$

Any command which causes the flux angle  $\vartheta_{sr}$  to change will determine a torque variation. In order to obtain high dynamic performance it is then necessary to vary  $\vartheta_{sr}$  quickly. This can be readily achieved acting on the angular speed of  $\vec{\varphi}_s^s$ .

Decoupled control of torque and stator flux can then be obtained acting respectively on the tangential and the radial components of  $\Delta\vec{\varphi}_s^s$ , defined with respect to the stator flux vector locus.

These two components are directly proportional to the components of  $\vec{v}_s^s$  in the same directions and can be controlled selecting the proper inverter switching configuration.

### Stator flux and torque estimation

Basically, DTC schemes require the estimation of stator flux and torque. The stator flux evaluation can be carried out by different techniques, depending on whether the rotor angular speed (or position) is measured or not. For sensorless applications the "voltage model" is usually employed. The stator flux can be evaluated by integrating from the stator voltage equation (1) according to

$$\vec{\varphi}_s^s = \int (\vec{v}_s^s - R_s \vec{i}_s^s) dt \quad (5)$$

This method is very simple requiring the knowledge of the stator resistance only. The effect of an error in  $R_s$  is usually quite negligible at high excitation frequency but becomes more serious as the frequency approaches zero [4]. Furthermore, at very low speed the open-loop integration (5) yields inaccurate results. Therefore, the speed range of the drive has a lower limit of about 5% of the rated speed.

When the rotor angular speed (or position) is available, the stator flux can be estimated with reference to the "current model". This method is based on the calculation of the rotor flux by the following equation

$$\vec{\varphi}_r^s = \int_0^t \left( \frac{M}{\tau_r} \vec{i}_s^s + jP\omega_m \vec{\varphi}_r^s - \frac{\vec{\varphi}_r^s}{\tau_r} \right) dt \quad (6)$$

The stator flux is then obtained from the rotor flux as follows

$$\vec{\varphi}_s^s = \frac{M}{L_r} \vec{\varphi}_r^s + \sigma L_s \vec{i}_s^s \quad (7)$$

The implementation of the rotor flux estimator based on (6) requires the knowledge of a greater number of parameters with respect to that based on (5). Furthermore Eq. 6 needs an accurate measurement of the speed. This can be shown rewriting (6) in steady-state conditions, leading to

$$\vec{\varphi}_r^s = \frac{M}{1 + j(\omega_s - P\omega_m)\tau_r} \vec{i}_s^s \quad (8)$$

Eq. 8 clearly shows that, owing to the small value of  $\omega_r = \omega_s - P\omega_m$ , even small percent errors in the measured speed determine not negligible errors in the rotor flux, particularly at high speed.

The combined use of "voltage model" and "current model" allows an accurate calculation of the rotor flux all over the speed range. In particular the first method is suitable at high speed, while the second at low speed. Several techniques have been proposed to combine the two methods. They are mainly based on algebraic [5] or dynamic procedures [2], [6].

With reference to the evaluation of the electromagnetic torque, the following equation can be usefully employed

$$T = P \vec{i}_s^s \cdot j\vec{\varphi}_s^s \quad (9)$$

This calculation requires the estimated value of the stator flux and no further machine parameters.

### Influence of the applied voltage on stator flux and torque

According to the principle of operation of DTC the selection of the proper voltage vector, at each sampling period, is made in order to maintain the torque and the stator flux within the limits of two hysteresis bands. In particular, the selection is made on the basis of the instantaneous errors in torque and stator flux. Assuming the stator flux vector lying in the  $k$ -th sector ( $k=1,2,3,4,5,6$ ) of the  $d$ - $q$  plane, in order to increase its magnitude the voltage vectors  $V_k, V_{k+1}, V_{k-1}$  can be selected (Fig. 2). Conversely, the decrease of  $\varphi_s$  can be obtained selecting  $V_{k+2}, V_{k-2}, V_{k+3}$ . The zero-voltage vector does not affect substantially the stator flux vector, with the exception of a small flux weakening due to the stator IR drop.

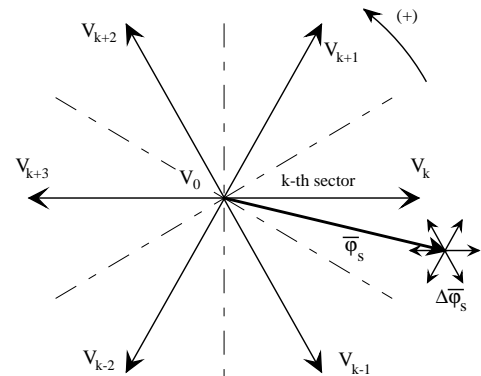


Fig. 2 - Inverter output voltage space vectors and corresponding stator flux variations in a period  $\Delta t$ .

For the following considerations the counter clockwise direction is assumed to be positive for space-vector rotation (Fig. 2), shaft speed and torque.

Of course, the voltage vectors utilised to control the stator flux affect the torque value also. Tab. I summarises the combined action of each configuration on both stator flux and torque. As it

appears evident, for both positive and negative shaft speed, an increment of torque ( $\uparrow$ ) is obtained selecting two voltage vectors only, that are  $V_{k+1}$  and  $V_{k+2}$ . Conversely, a decrement of torque ( $\downarrow$ ) can be achieved utilising  $V_{k-1}$  or  $V_{k-2}$ . The radial voltage vectors  $V_k$ ,  $V_{k+3}$  and the zero voltage vector  $V_o$  act on the torque in accordance to the mechanical speed direction as it is specified in Tab. I. In this table, a single arrow specifies small influence on flux or torque increments, while two arrows denote larger influence.

TABLE I - FLUX AND TORQUE VARIATION DUE TO THE APPLIED VOLTAGE VECTORS

	$V_{k-2}$	$V_{k-1}$	$V_k$	$V_{k+1}$	$V_{k+2}$	$V_{k+3}$	$V_o$
$\phi_s$	$\downarrow$	$\uparrow$	$\uparrow\uparrow$	$\uparrow$	$\downarrow$	$\downarrow\downarrow$	$\uparrow\downarrow$
$T$ ( $\omega_m > 0$ )	$\downarrow\downarrow$	$\downarrow\downarrow$	$\downarrow$	$\uparrow$	$\uparrow$	$\downarrow$	$\downarrow$
$T$ ( $\omega_m < 0$ )	$\downarrow$	$\downarrow$	$\uparrow$	$\uparrow\uparrow$	$\uparrow\uparrow$	$\uparrow$	$\uparrow$

The hysteresis band technique, applied to control stator flux and torque, leads to four possible conditions regarding to the instantaneous errors. For each condition it is possible to find one voltage vector at least which allows the torque and flux errors to be reduced. It is then possible to drive stator flux and torque to follow any desired track curve. This allows decoupled control of flux and torque to be achieved.

#### Analysis of different switching strategies

in the previous section it has been shown that, for any combination of the required flux and torque increments, various voltage vectors can be selected. the choice of one of them is made on the basis of prefixed selection strategies. each strategy affects the drive behaviour in terms of torque and current ripple, switching frequency, dynamic performance and two- or four-quadrant operation capability.

#### Two-quadrant operation

For positive mechanical speed, only two voltage vectors can be selected to increase the torque, that are  $V_{k+1}$  or  $V_{k+2}$  according to the stator flux requirements. In order to decrease the torque it is possible nearly to stop the stator flux vector rotation using radial ( $V_k$  or  $V_{k+3}$ ) or zero voltage vectors ( $V_o$ ). The strategies based on the selection of these voltage vectors are summarised in Tab. II

TABLE II - SELECTION STRATEGIES FOR TWO-QUADRANT OPERATION

	$T \uparrow$	$T \downarrow$		
		A	B	C
$\phi_s \uparrow$	$V_{k+1}$	$V_o$	$V_k$	$V_k$
$\phi_s \downarrow$	$V_{k+2}$	$V_o$	$V_o$	$V_{k+3}$

The action of zero or radial voltages on torque variation is quite similar. Note that, being the torque variation related to the rotor angular frequency, the torque response degrades at low speed. Zero and radial voltage vectors have different influence on flux variations. In particular, the use of zero voltage vectors determines small flux magnitude variations, while the radial vectors strongly affect the flux magnitude. As a consequence, in this last case, to keep the stator flux within the hysteresis band a greater number of commutation is required. Then, in order to limit the switching frequency it should be opportune to use zero voltage vectors [2], [3]. On the other hand, at low speed, the control system selects many times zero voltage vectors. This, together with the influence of stator IR drop, causes undesired flux

weakening. To avoid this drawback, when a torque decrease is required, in order to increase the flux magnitude it is opportune to select the radial vector  $V_k$ .

All the strategies based on Tab. II allow two-quadrant operation only, because the use of forward voltage vectors together with zero or radial vectors leads to positive values of  $\omega_s$ . However, it should be noted that the condition  $\omega_s \geq 0$  imposes a lower limit to the torque at low speed. In fact, considering the torque expressed in terms of rotor flux and rotor angular frequency

$$T = P \frac{\omega_r}{R_r} \phi_r^2 \quad (10)$$

and introducing the steady-state condition  $\omega_s = P\omega_m + \omega_r \geq 0$ , leads to

$$T \geq -P^2 \frac{\omega_m}{R_r} \phi_r^2 \quad (11)$$

Eq. 11 gives analytically the lower limit for the torque values. This limit is particularly important at very low speed.

#### Four-quadrant operation

To improve the dynamic performance of DTC at low speed and to allow four-quadrant operation, it is necessary to involve the voltage vectors  $V_{k-1}$  and  $V_{k-2}$  in torque and flux control. In the following,  $V_{k-1}$  and  $V_{k-2}$  will be denoted "backward" voltage vectors in contraposition to "forward" voltage vectors utilised to denote  $V_{k+1}$  and  $V_{k+2}$ . A simple strategy which makes use of these voltage vectors is shown in Tab. III.

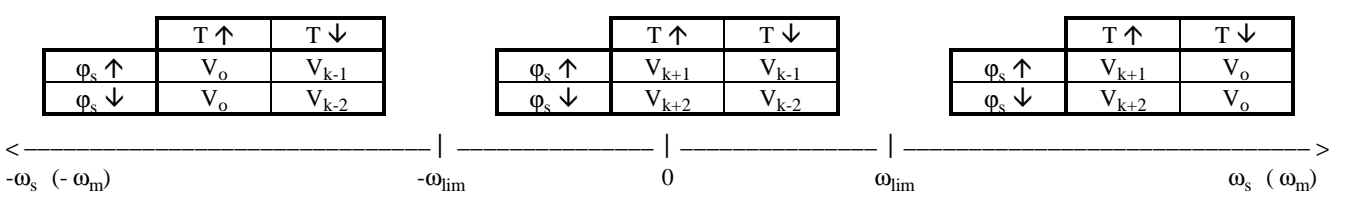
TABLE III - SELECTION STRATEGY FOR FOUR-QUADRANT OPERATION

	$T \uparrow$	$T \downarrow$
$\phi_s \uparrow$	$V_{k+1}$	$V_{k-1}$
$\phi_s \downarrow$	$V_{k+2}$	$V_{k-2}$

According to this strategy the stator flux vector is required to rotate in both positive and negative directions. By this, even at very low shaft speed, large negative values of rotor angular frequency can be achieved, which are required when the torque is to be decreased very fast. Furthermore, the selection strategy represented in Tab III allows good flux control to be obtained even in the low speed range. However, the high dynamic performance which can be obtained utilising voltage vectors having large components tangential to the stator vector locus implies very high switching frequency.

A control techniques has been proposed in [2] which utilises zero and forward voltage vectors, leaving the use of backward voltage vectors only during abrupt decrease of torque command and for mechanical speed reversal. This is obtained introducing a three-level hysteresis control. In particular, when the torque exceeds the upper or the lower limit, backward or forward vectors are applied respectively in order to obtain fast torque response. When the torque crosses the central limit (set point), a zero voltage vector is selected in order to obtain low switching frequency. In this way, the torque varies inside the lower or the upper band with forward or backward mechanical speed respectively, allowing four-quadrant operations. However, this solution does not avoid undesired flux weakening at low speed due to the use of zero voltage vector, as previously explained. Furthermore, when implementing digitally this control technique, the actual torque systematically exceeds both upper and lower limits even in steady-state operation. This leads to the typical behaviour of a two-level hysteresis control which utilises forward and backward voltage vectors only (see Table III). To overcome this drawback the band amplitude could be increased, but this obviously determines higher torque ripple. It should be noted also that the increase of the band amplitude in three-level hysteresis control determines larger difference between the torque mean values corresponding to positive and negative mechanical speeds.

TABLE IV - SPEED-DEPENDENT SELECTION STRATEGY



In more recent papers a hysteresis torque control based on two centred bands has been proposed [7], [8]. The inner band is used to control the torque according to the selection strategy represented in Tab. II-B. The outer band is used to select forward or backward voltage vectors in order to obtain high dynamic response and four-quadrant operation capability. This control technique determines torque oscillations between inner and outer bands during torque step response and mechanical speed reversal. This behaviour could be critical in position control systems.

### Analysis of a new switching strategy

As previously discussed, the effect of the applied voltage on the torque response is strongly dependent on rotor angular speed. At low speed, forward and backward voltage vectors determine nearly the same absolute value of rotor angular frequency. This allows quick torque response to be obtained for both increase or decrease of torque command. Conversely, the use of zero and radial voltage vectors results in slow torque response. Consequently, at low speed, it is opportune to utilise forward and backward voltage vectors, so avoiding flux weakening phenomena also.

At high positive (negative) speed the use of backward (forward) voltage vectors should be avoided because they determine too large values of the rotor angular frequency. As a consequence, the torque changes too quickly leading to high switching frequency. Good dynamic performance and substantial reduction of the switching frequency can be achieved selecting forward and zero voltage vectors. Furthermore, being the zero voltage vector selected fewer times than forward voltage vectors, flux weakening phenomena are avoided.

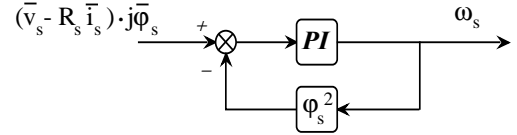
The use of radial voltage vectors is not necessary because in spite of quick flux response, high switching frequency is obtained.

From these considerations it is possible to individuate a new switching strategy, which is based on the use of forward and backward voltage vectors in the low speed range only (say, 20% of rated speed). For high positive rotor speed, zero and forward voltage vectors can be suitable utilised, as well as zero and backward voltage vectors for high negative rotor speed. This new switching strategy is summarised in Tab. IV. When implementing this vector selection technique, it is necessary to know the rotor speed value  $\omega_m$ . If the "current model" is used for flux estimation,  $\omega_m$  is already available. In sensorless applications, based on "voltage model", the stator angular frequency  $\omega_s$  can be usefully employed instead of  $\omega_m$  in order to determine the different speed ranges. In fact, the estimation of  $\omega_s$  is easier than that of  $\omega_m$  and its use in finding the speed range does not introduce drawbacks. The stator angular frequency can be estimated by the following equation

$$\omega_s = \frac{(\bar{v}_s - R_s \bar{i}_s) \cdot j\bar{\phi}_s}{\phi_s^2} \quad (12)$$

Eq. 12 gives the instantaneous value of  $\omega_s$  which contains high frequency harmonic components. The average value of  $\omega_s$ , required to actuate the proposed switching strategy, can be evaluated according to the block diagram of Fig. 3. In this way, the value of  $\omega_s$  is obtained without performing the ratio in Eq. 12

and the low-pass filtering action of the PI regulator gives the desired averaging function.

Fig. 3 - Block diagram for the evaluation of  $\omega_s$ .

### Experimental results

A complete torque controlled drive system, using DTC scheme, has been realised. The proposed control technique is based on the combination of three voltage vector selection strategies, one valid in low speed range and the others in high speed range (Tab. IV). The goal is the direct and independent control of stator flux and torque, with four-quadrant operation capability, while keeping the switching frequency at the lowest value compatible with good dynamic performance. With reference to a sensorless application, the "voltage model" has been adopted to estimate the stator flux. Then, the switching strategy is selected on the basis of the estimated stator flux angular frequency, while the switching configuration is determined by the stator flux and torque errors and the angular sector (k) in which the stator flux lies. Utilising the same control system all the switching strategies previously described can be also implemented and tested.

The experimental set-up includes a fully digital controlled IGBT inverter and a 4 kW, 220V, 50 Hz, 4-poles standard induction motor.

For the implementation of the different control strategies, a DSP-based processing system has been chosen. A 4-channel 12-bit A/D converter allows to read in the DC voltage, two line currents and the torque command. The quantities calculated by the digital controller can be selected and read out through two 12-bit D/A converters. The low computational time required to implement the DTC on a fixed point DSP (TMS320-15), allows 20 kHz sampling frequency including stator flux angular frequency estimation, overcurrent protection and diagnostic facility. Various tests have been carried out to compare the different switching strategies and to characterise their transient performance.

First, the steady-state behaviour has been investigated considering the switching strategies represented in Tab. II-A, Tab. II-B, Tab. II-C and Tab. III. Fig. 4 shows the stator flux vector loci obtained using the same hysteresis band amplitude. With reference to the results obtained utilising Tab. II, it can be seen the increase of the switching frequency when the radial voltage vectors are selected instead of zero voltage vectors. The vector locus relative to Tab. III denotes irregularities due to the combined use of forward and backward voltage vectors.

The transient behaviour has been tested applying a pulse change in torque command from 18 Nm to -18 Nm, for a period of 8.8 ms. The torque responses obtained at low and high speed are illustrated in Figs. 5 and 6 respectively. Owing to the large load inertia, the rotor speed remains practically unchanged during the transient. Top traces refer to the switching strategy of Tab. III while bottom traces refer to the switching strategy of Tab. II-A.

*Ref. to Tab. II-A*

*Ref. to TabII-B*

*Ref. to Tab. II-C*

*Ref. to Tab. III*

*Fig. 4 - Experimental stator flux vector loci using different switching strategies. Rated torque and flux,  $\omega_m=100$  rad/s.*

These traces clearly show the influence of the two switching strategies on the torque response, depending on the operating speed. Note the slow torque response when utilising zero voltage vectors at low speed. On the contrary, at high speed, the torque response of the two switching strategies is quite similar.

The proposed control system utilizes the switching strategy of Tab. IV with  $\omega_{lim}=30$  rad/s. The transient performance of the experimental drive has been tested applying to the control system a torque reference alternating between  $\pm 18$  Nm with a frequency of 0.26 Hz. The motor is coupled to a large inertial load and the resulting speed range is  $\pm 100$  rad/s. The experimental results are given in Figs. 7 and 8. In Fig. 7 the top and bottom traces represent the estimated torque and the measured rotor speed respectively. Owing to display resolution, it is not possible to see how the torque ripple changes in the different speed ranges. However, details about torque ripple at different speeds are illustrated in Fig. 5 and 6. The speed irregularities are due to the critical estimation of the flux and torque at very low speed (voltage model).

In Fig. 8 the top trace represents the estimated torque in the same operating conditions as in Fig. 7, but with expanded time scale. The bottom trace shows the stator current waveform. The small perturbations in the torque trace correspond to changes of the switching strategy.

### **Conclusions**

This paper has presented a control scheme for direct torque control of induction machines which utilises a new switching strategy. The influence of different voltage vector selection criteria on stator flux and torque ripple has been firstly discussed in order to emphasise the different drive behaviour at low and high speed. In particular it has been shown that the use of zero voltage vectors together with backward or forward voltage vectors has the advantage of low switching frequency. However, at low speed it causes undesired flux weakening phenomena and limits in dynamic performance.

On the other hand the use of forward and backward voltage vectors only, in spite of high dynamic performance all over the speed range, leads to high switching frequency. These problems are overcome in the proposed scheme by using different switching strategies at low and at high speed. This, of course, implies the knowledge of the mechanical speed. In drive systems not equipped with rotational transducer the estimation of the rotor angular speed should be performed. However, it has been shown that the estimation of the stator angular frequency can be usefully employed instead of rotor speed.

The experimental results show that good performance of the drive system is accomplished in steady state as well as under transient conditions.

*Tab. III*

*Tab. II-A*

*Fig. 5 - Torque response to a pulse change in torque command from +18 to -18 Nm,  $\Delta T=8.8$  ms,  $\omega_m=20$  rad/s.*

*Fig. 6 - Torque response to a pulse change in torque command from +18 to -18 Nm,  $\Delta T=8.8$  ms,  $\omega_m=100$  rad/s.*

Fig. 7 - Dynamic response of the experimental drive to a torque command alternating between  $\pm 18$  Nm. Top trace: estimated torque. Bottom trace: mechanical speed.

Fig. 8 - Dynamic response of the experimental drive to a torque command alternating between  $\pm 18$  Nm. Top trace: estimated torque. Bottom trace: stator current.

### Nomenclature

$p$	differential operator (d/dt)
$P$	pole pair
$s,r$	superscript denoting stator, rotor reference frame
$s,r$	subscripts denoting stator and rotor quantities
$L,M$	self- and mutual inductance
$R$	phase resistance
$\sigma = 1 - \frac{M^2}{L_s L_r}$	total leakage coefficient
$\tau_r = L_r / R_r$	rotor time constant
$\omega_s$	stator flux angular frequency
$\omega_r$	rotor flux angular frequency
$\omega_m$	mechanical shaft angular speed
$T$	electromagnetic torque
$\underline{x} = x_d + jx_q$	space vector representation
$\varphi$	linkage flux
$i$	phase current
$v$	phase voltage
$V_k$	inverter output voltage vector lying in k-th sector

### References

- [1] D. Casadei, G. Grandi, G. Serra: *Study and implementation of a simplified and efficient digital vector controller for induction motors*. IEE Conf. Pub. No 376, EMD'93, Oxford, UK, 8-10 September 1993, Proc. pp. 196-201.
- [2] I. Takahashi, T. Noguchi: *A new quick-response and high-efficiency control strategy of an induction motor*. IEEE Trans. on IA, Vol. 22, No. 5, Sept/Oct 1986, pp. 820-827.
- [3] M. Depenbrok: *Direct Self-Control (DSC) of Inverter-Fed Induction Machine*, IEEE Trans. on Power Electronics. Vol. 3, N. 4, October 1988, pp. 420-429.
- [4] D. Casadei, G. Grandi, G. Serra: *Rotor flux oriented torque-control of induction machines based on stator flux vector control*. IEE Conf. Pub. No 377. EPE'93, Brighton UK, 13-16 September 1993, Proc. Vol. 5, pp. 67-72.
- [5] F. Profumo, A. Tenconi, R.W. De Donker: *The universal field oriented (UFO) controller applied to wide speed range induction motor drives*, PESC-1991, Boston USA, pp.681-686.
- [6] T. Svensson, M. Alakula: *The modulation and control of a matrix converter synchronous machine drive*, EPE-1991, Firenze (I), Vol. 4, pp. 469-476.
- [7] I. Takahashi, T. Kanmachi: *Ultra-wide speed control with a quick torque response AC servo by a DSP*. EPE '91, Florence, Italy, September, 3-6 1991, Proc. Vol. III, pp. 572 - 577.
- [8] I. Takahashi, Y. Ide: *Decoupling Control of Thrust and Attractive Force of a LIM Using a Space Vector Control Inverter*. IEEE Trans., Vol. IA-29, N. 1, Jan/Feb 1993, pp. 161-167.